J Plant Growth Regul (2014) 33:328–339
DOI 10.1007/s00344-013-9379-8

Carbon-11 Reveals Opposing Roles of Auxin and Salicylic Acid in Regulating Leaf Physiology, Leaf Metabolism, and Resource Allocation Patterns that Impact Root Growth in *Zea mays*

Beverly Agtuca · Elisabeth Rieger · Katharina Hilger · Lihui Song · Christelle A. M. Robert · Matthias Erb · Abhijit Karve · Richard A. Ferrieri

Received: 25 April 2013 / Accepted: 3 September 2013 / Published online: 18 October 2013

Abstract Auxin (IAA) is an important regulator of plant development and root differentiation. Although recent studies indicate that salicylic acid (SA) may also be important in this context by interfering with IAA signaling, comparatively little is known about its impact on the plant's physiology, metabolism, and growth characteristics. Using carbon-11, a short-lived radioisotope ($t_{1/2} = 20.4$ min) administered as $^{11}CO_2$ to maize plants (B73), we measured changes in these functions using SA and IAA treatments. IAA application decreased total root biomass, though it increased lateral root growth at the expense of primary root elongation. IAA-mediated inhibition of root growth was correlated with decreased $^{11}CO_2$ fixation, photosystem II (PSII) efficiency, and total leaf carbon export of ^{11}C-photoassimilates and their allocation belowground. Furthermore, IAA application increased leaf starch content. On the other hand, SA application increased total root biomass, $^{11}CO_2$ fixation, PSII efficiency, and leaf carbon export of ^{11}C-photoassimilates, but it decreased leaf starch content. IAA and SA induction patterns were also examined after root-herbivore attack by *Diabrotica virgifera* to place possible hormone crosstalk into a realistic environmental context. We found that 4 days after infestation, IAA was induced in the midzone and root tip, whereas SA was induced only in the upper proximal zone of damaged roots. We conclude that antagonistic crosstalk exists between IAA and SA which can affect the development of maize plants, particularly through alteration of the root system's architecture, and we propose that the integration of both signals may shape the plant's response to environmental stress.

Keywords Carbon-11 · PET imaging · Auxin · Salicylic acid · Hormone crosstalk · Root–herbivore interactions

B. Agtuca
State University of New York College of Environmental Science and Forestry, Syracuse, NY 13210, USA

E. Rieger · K. Hilger
Fachbereich Chemie, Johannes Gutenberg Universität, 55099 Mainz, Germany

L. Song
Plant Sciences Division, Department of Chemistry, Bond Life Sciences Center, University of Missouri, Columbia, MO 65211, USA

C. A. M. Robert · M. Erb
Root-Herbivore Interactions Group, Max Planck Institute for Chemical Ecology, Hans-Knöll-Str. 8, 07745 Jena, Germany

C. A. M. Robert
Department of Biochemistry, Max Planck Institute for Chemical Ecology, Hans-Knöll-Str. 8, 07745 Jena, Germany

A. Karve · R. A. Ferrieri (✉)
Biosciences Department, Brookhaven National Laboratory, Building 901, Upton, NY 11973, USA
e-mail: rferrieri@bnl.gov

Introduction

Increased demand for both energy and food driven by an increasing global population is causing continual depletion of precious land resources. Left unchecked, these demands will soon require an agroeconomy that can be sustainable on marginal land. To survive these conditions, cropping systems will need to be vigorous competitors with root systems that are capable of foraging for limited water and limited nutrients (Hodge 2004). Root growth is perhaps the most important agronomic trait underpinning a plant's hardiness to grow during times of stress as it defines how

well that plant can maintain a steady supply of water and nutrients from belowground, enabling its aboveground tissues and organs to function optimally (Cahill and McNickle 2011; Kumar and others 2012). Root systems also play an integral role in regulating overall plant defenses, enabling the plant to better cope with the stresses imposed by predators and/or pathogens both aboveground (Ferrieri and others 2012; Machado and others 2013) and belowground (Rasmann and others 2005).

Plants use long-range signaling involving hormones to coordinate growth and defense responses among the distal tissues and organs of the plant (Thorpe and others 2007). Hormones such as salicylic acid (SA) play important roles in inducing plant resistance against biotrophic pathogens and some phloem-feeding insects (Shah 2003; Durrant and Dong 2004; Vlot and others 2009). Others like jasmonic acid can induce resistance against necrotrophic pathogens, some phloem-feeding insects, and chewing herbivores (Wasternack 2007; Truman and others 2007). Yet other hormones are known classically for their role in regulating basic plant functions that underpin growth, including the physiological and metabolic responses of the plant (Buchanan and others 2000).

Auxin (IAA) is a plant hormone that falls into this latter category. It is best known for its diverse roles in regulating developmental and cellular processes impacting axis formation and patterning during post-embryogenesis, vascular elongation, leaf expansion, inflorescence, fruit development, tropism, and apical dominance (Woodward and Bartel 2005; Kazan and Manners 2009). Auxin is also especially important in regulating root development (McSteen 2010). Most particularly, it will cause extensive lateral root patterning and root hair formation, but at the expense of root elongation.

As with any hormone, the signaling network of a single hormone does not occur in isolation, but in concert with the presence, and actions, of other hormones. This makes it extremely difficult to delineate the role of that single hormone when others may also be impacting plant function at the same time. Furthermore, plant hormones may serve multiple roles. For example, whereas auxin is widely known for its role in growth regulation, there is evidence suggesting that it may also regulate plant defenses (Kunkel and Brooks 2002; Katagiri 2004). SA has also been implicated as having multiple functions in plants (Park and others 2007; Rivas-San and Plasencia 2011). In addition to its role in plant defense, SA has been tied to regulating seed germination, seed production, leaf senescence, photosynthesis, respiration, thermogenesis, and flower formation (Hayat and others 2007). In addition to impacting basic plant functions, SA can affect root phenotypes such as root patterning (Li and Li 1995; Gutierrez-Coronado and others 1998; Echevarria-Machado and others 2007).

There is also clear evidence which demonstrates that crosstalk exists between SA and IAA at a molecular level (for a review, see Spoel and Dong 2008). SA binds to AUX/IAA repressor proteins, preventing their destabilization during auxin signaling and essentially short-circuiting the auxin signal network (Zhang and others 2007; Llorente and others 2008). Certain Dof domain proteins, including OBP1, OBP2, and OBP3, which are induced by SA in *Arabidopsis*, are also responsive to auxins (Kang and Singh 2000).

The purpose of this research was to explore the individual effects of SA and IAA treatments on whole-plant physiology, plant carbohydrate metabolism, and terminal phenotypes of root growth in *Zea mays*. We hypothesized that treatment with these hormones would have opposite effects on these basic plant functions and on terminal phenotypes. Our investigations made use of the core capabilities at Brookhaven National Laboratory's Plant Radiotracer Laboratory, enabling us to administer discrete doses of radioactive $^{11}CO_2$ to intact plants to measure its fixation by leaves, its incorporation into ^{11}C-photosynthates, and their export to distal tissues/organs (Minchin and Thorpe 2003; Ferrieri and others 2005). Using a combination of positron emission tomography (PET) and autoradiography, we were able to visualize and quantify the dynamic transport of ^{11}C-photosynthates from leaves to roots (Fig. 1). Bioassays were also applied to measuring $^{11}C/^{12}C$ isotopic signatures in key metabolite pools, providing insight into metabolic fluxes of new carbon as ^{11}C relative to turnover of storage carbon. This combination of imaging with radiometric bioassays provided a powerful investigational tool for measuring the effects of hormones on whole-plant physiology and on plant metabolism and relating changes in these basic plant functions with growth and development.

Lastly, we wanted to explore the in vivo regulation of IAA and SA hormones in a biologically relevant context that closely associates with real-world conditions that plants may experience in the environment. We used feeding by the specialist root herbivore *Diabrotica virgifera* as a way to leverage changes in the endogenous root hormone levels to determine whether local root tissues exhibit opposite induction patterns in IAA and SA.

Materials and Methods

Materials

All chemicals used in these studies were obtained from Sigma-Aldrich (St. Louis, MO, USA) and were used without any further purification.

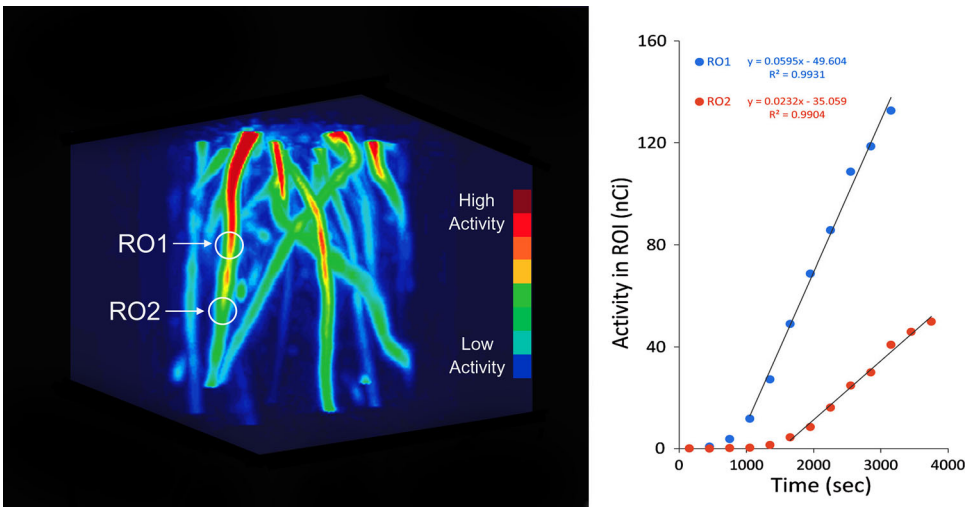

Fig. 1 ROIs were drawn on reconstructed PET images using ASIPro VM software, and time-of-arrival within ROIs was calculated from time–activity curves using regression analysis

Plant Growth and Treatment

Corn kernels of the B73 line (USDA Agricultural Resource Services—Germplasm Resource Network, Ames, IA, USA) were germinated in darkness for 48 h on wetted KimWipe™ tissues placed in 7 × 7-cm Petri dishes. The dishes were wrapped with aluminum foil and kept at room temperature. After 48 h the Petri dishes were unwrapped and placed under Agro lights giving 100 µmol m^{-2} s^{-1} of light intensity during a 16-h photoperiod. When the primary root of a germinating seedling reached 1–2 cm in length, the seedling was transplanted into a 600-mL glass growth cell filled with Hoagland's fortified agar gel.

Agar gels were prepared out of 3 L of deionized water, 4.9 g Hoagland modified basal salt mixture (PhytoTechnology Laboratories, Shawnee Mission, KS, USA), and 1.66 g MES hydrate. The pH of the solution was adjusted to 5.9 by adding 1 N sodium hydroxide solution. While stirring, 8.4 g Gelzan CM (Sigma-Aldrich) was added. The solution was autoclaved (Harvey SterileMax, Thermo Fisher Scientific, Pittsburgh, PA, USA) for 15 min at 121 °C and mixed at high speed to enable aeration of the viscous solution before it had a chance to set as a gel. Treatments, including 1,140 nM IAA and 1,500 nM SA, were introduced to the solution during the aeration stage once the temperature of the mixed solution dropped below 40 °C. Treatment concentrations were based on prior published work (Baker and Ray 1965; Li and Li 1995). Control studies were identical to those described above with the exception that no IAA or SA was added to the agar gel. Sterilized plastic inserts were placed within each cell before the gel set. This allowed us to position the germinated kernel into a notch in the top portion of the cell. Following this, the tops of the cells were sealed with Parafilm™ and completely wrapped with aluminum foil to block out light. A small hole at the top of the cell enabled the developing plant to grow through. The cells were cultivated in growth chambers (Conviron, Inc., Winnipeg, MB, Canada) at 23 °C using 320 µmol m^{-2} s^{-1} of light intensity on a 12-h photoperiod. Three-week-old plants that measured ~35–40 cm in height were used for studies.

For root herbivory by *D. virgifera*, plants were grown in the greenhouse (24 ± 2 °C, 14 h light/10 h dark, 55-% relative humidity) in 1-L pots (5.5-in. o.d. × 3.5-in. height) filled with washed sand (0.7–1.2 mm, Hagebaumarkt Leipzig GmbH, Leipzig, Germany) topped with soil (Klasmann Tonsubstrat, Geeste, Germany). Three-week-old plants were subjected to root herbivory by 12 *D. virgifera* larvae at their second instar stage. Larvae were allowed to feed for 4 days prior to tissue collection for hormone analysis.

Radiotracer Production and Tracer Administration

$^{11}CO_2$ was produced via the $^{14}N(p, \alpha)^{11}C$ nuclear transformation (Ferrieri and Wolf 1983) from a 20-mL target filled with high-purity nitrogen gas (400 mL @ STP) using 18-MeV protons from the TR-19 (Ebco Industries Ltd, Richmond, BC, Canada) cyclotron at BNL and captured on a molecular sieve (4 Å). The $^{11}CO_2$ that was trapped on the molecular sieve was desorbed and quickly released into an air stream at 200 mL min^{-1} as a discrete pulse for labeling a leaf affixed within a 5 × 10-cm lighted (320 µmol m^{-2} s^{-1}) leaf cell at 21 °C to ensure a steady level of fixation. The load leaf affixed within the cell was pulse-fed $^{11}CO_2$ for 1 min, then chased with normal air for the duration of exposure. A PIN diode radiation detector (Carroll Ramsey Associates, Inc, Berkeley, CA, USA) affixed to the bottom of the leaf cell enabled continuous measurement of radioactivity levels within the cell during the initial pulse and in the minutes right after the pulse, giving information on $^{11}CO_2$ fixation.

Physiological Measurements

Four physiological parameters were measured in our tracer studies: (1) leaf photosynthesis, including $^{11}CO_2$ fixation, and parameters of the light reactions, including chlorophyll fluorescence (F), photosystem (II) (PSII) quantum efficiency, and nonphotochemical quenching (NPQ); (2) leaf export of ^{11}C-photosynthates; (3) allocation patterns of ^{11}C-photosynthates between above- and belowground tissues, as well as allocation patterns within targeted lateral roots and their parent root sections; and (4) the rate of ^{11}C-photosynthate transport within roots.

Prior to radiotracer studies, plants were subjected to 2D fluorescence imaging using the Maxi version of the Walz Imaging PAM system (Heinz Walz GmbH, Effeltrich, Germany). Measurements were made at the end of the dark cycle in attached leaves to obtain minimal fluorescence (F_0) and maximal fluorescence yields (F_m) in dark-adapted samples. F_0 was measured at low frequency of pulse-modulated measuring light, while F_m was measured using a saturation pulse. This was followed by 2-min exposure at 280 µmol m^{-2} s^{-1} PAR, with measurements of F, the fluorescence yield, integrated across three defined regions of the leaf. The PSII and NPQ levels were automatically calculated by the ImagingWin software using Eqs. 1 and 2:

$$\text{PSII} = \frac{(F'_m - F)}{F'_m} \tag{1}$$

$$\text{NPQ} = \frac{(Fm - F'_m)}{F'_m} \tag{2}$$

We used microPET imaging (Concorde MicroSystems, Inc., Knoxville, TN, USA) to carry out 90-min dynamic scanning on roots. ASIPro VM software (RSI Research Systems, Inc., Boulder, CO, USA) was used to create regions of interest (ROI) on reconstructed images, giving information on radioactivity time-of-arrival between those ROIs. Distances between ROIs were also measured in pixels using the same software and related to millimeter spatial scales for calculating velocities (mm min^{-1}). After the microPET imaging, plants were removed from their growth cells and selected crown roots were imaged using autoradiography (Typhoon 7000: GE Healthcare, Piscataway, NJ, USA). These data were later used to calculate distributions of radioactivity within lateral roots and their parent roots using ImageQuant TL 7.0 software (GE Healthcare BioSciences AB, Uppsala, Sweden).

Afterward, plant tissues were further dissected into load leaf tissue, shoots/stems, and remaining roots and counted for radioactivity levels using a Capintec Radioisotope Dose Calibrator CRC-12 (Capintec, Inc, Ramsey, NJ, USA). Radioactivity was corrected for decay using the end-of-bombardment time as time zero. Leaf export values were calculated using Eq. 3:

$$\text{Fractional leaf export} = 1 - \left(\frac{\text{Load leaf activity}}{\text{Activity (load leaf + shoots + stem + roots)}}\right) \tag{3}$$

Belowground allocation values were calculated using Eq. 4:

$$\text{Belowground allocation} = \left(\frac{\text{Root activity}}{\text{Activity(shoots + stem + roots)}}\right) \tag{4}$$

After imaging and tissue counting, the shoots, stems, and roots (including a subset of lateral roots and their parent root sections) were dried for 48 h in an oven (Thelco Oven, Thermo Fisher Scientific, Inc., Pittsburgh, PA, USA) at 55 °C, and dry mass was measured for tissue normalization of whole-plant photosynthate allocation. From the subset of lateral root, and respective parent root data, we were able to calculate the relative lateral root sink strength for ^{11}C-photosynthate using Eq. 5 (values were normalized to an average control value equal to 1.0):

$$\text{Relative lateral root sink strength} = \left[\frac{\left[\frac{\text{Lateral root activity}}{\text{Lateral root dry mass}}\right]}{\left[\frac{\text{Parent root activity}}{\text{Parent root dry mass}}\right]}\right]_{\text{Treatment}} \times \left[\frac{\left[\frac{\text{Parent root activity}}{\text{Parent root dry mass}}\right]}{\left[\frac{\text{Lateral root activity}}{\text{Lateral root dry mass}}\right]}\right]_{\text{Control}} \tag{5}$$

Tissue Extraction and Carbohydrate Analysis

A smaller portion of the load leaf tissue was immediately frozen in liquid nitrogen and ground by hand in a preweighed and prechilled Eppendorf™ tube. The tissue was extracted in 4× w/v of methanol, briefly vortexed (VWR analog vortex mixer; Sigma-Aldrich), and then sonicated (Branson Bransonic 32; Sigma-Aldrich) in an iced water bath for 10 min with intermittent vortexing to ensure complete mixing. The tubes were centrifuged (Eppendorf Centrifuge 5424) for 2 min at 15,000 rpm and the supernatant was filtered through 0.2-µm Acrodiscs (Gelman Sciences, Ann Arbor, MI, USA). The pellet contained all insoluble components which comprised mostly cell-wall polymers and starch. The filtrate contained small soluble compounds, including soluble sugars. These sugars were separated and analyzed by thin layer chromatography (TLC) (Klaus and others 1989; Babst and others 2013). Glass-backed NH_2-silica HPTLC plates (200 µm, w/UV254) were used for the sugar separation

(Sorbent Technologies, Atlanta, GA, USA). Plates were prespotted with 1 μL sugar standards (5, 4, 2, 1, 0.5, and 0.25 mM of glucose, sucrose, and fructose) and 1- and 2-μL aliquots of leaf extract using a semiautomatic Linomat 5 sample applicator (Camag Scientific Inc., Wilmington, NC, USA) for high precision of spot size and sample volume. The larger volume of extract was sometimes needed to visualize the ^{11}C or ^{12}C hexose sugars, which were usually lower in concentration than sucrose. TLC plates were developed using a mobile phase consisting of 75:25 acetonitrile:water (v/v). Developed plates were imaged using autoradiography to determine the fraction of each radiolabeled sugar. The plates were then heat-treated (200 °C for 10 min) to initiate the chemical reaction of individual sugars with the amino functionalized silica-support that gave fluorescence under long-wavelength (365 nm) UV light (Klaus and others 1990). Digital photographs of the fluorescent markers were used to determine the ^{12}C-sugar concentration. ImageQuant TL software 7.0 (GE Healthcare BioSciences) was used to analyze both the radiographic and the digital images to determine the $^{11}C/^{12}C$ isotopic ratio within the individual sugars. Linear regression was used for standard curves generated from ^{12}C-sugar standards.

For starch measurement, leaf tissue was flash frozen in liquid nitrogen and ground to fine powder in 2-mL microcentrifuge tubes using Retsch Miximill MM400 (Retsch GmbH, Haan, Germany). Total starch was determined from the preweighed samples using a starch assay kit (Sigma-Aldrich) by following manufacturer's protocol with some modifications. Preweighed samples were incubated with 2 mL of 80 % methanol at 85 °C for 5 min followed by centrifugation. Methanol extraction was repeated twice to remove all the soluble sugars. The resulting pellet was digested using 100 U of α-amylase (supplied with the kit) at 96 °C for 10 min in a total reaction volume of 644 μL. The digest was then diluted to 2 mL with DI water and 100 μL of it was used for the next step. Each tube containing 100 μL digested sample was incubated with equal volume of starch assay reagent containing 5 U of amyloglucosidase at 60 °C for 15 min. The tubes were spun down at 15,000 rpm for 2 min and the resulting supernatant was analyzed by TLC to determine the concentration of the glucose derived from the starch digestion. Glass-backed NH_2-silica HPTLC plates (200 μm, w/UV254) were used for the sugar separation (Sorbent Technologies). Plates were prespotted with 1 μL glucose standards (0.25, 1.25, 2.5, 4, 5, and 7.5 mM glucose) and 2 μL starch digest using a semiautomatic Linomat 5 sample applicator (Camag Scientific Inc.). TLC plates were developed using a mobile phase consisting of 75:25 acetonitrile:water (v/v), developed and visualized as described previously for ^{12}C-sugar analysis. Image Quant TL software was used to analyze the digital images. A standard curve generated using a linear regression model was used to estimate the concentration of glucose from the digest. Starch content was expressed as glucose equivalents per gram of fresh weight.

Root Hormone Analysis

Plant material was ground into a fine powder in liquid nitrogen. IAA was extracted from 100 mg fresh plant material by adding 1 mL ethanol:acetic acid (99.5:0.5) containing hormone standards [10 ng IAA, 40 ng D_4-SA, and 40 ng JA (Santa Cruz Biotechnology, Santa Cruz, CA, USA] following procedures described in Vadassery and others (2012) and modified by Machado and others (2013). All samples were vortexed for 10 min, then centrifuged at 14,000 rpm for 20 min at 4 °C. The supernatants were collected and evaporated to dryness in a SpeedVac at room temperature (Eppendorf 5301). Pellets were then resuspended in 50 μL of methanol:water (70:30).

IAA was quantified by liquid chromatography using an Agilent 1260 Infinity HPLC system (Agilent Technologies, Inc., Santa Clara, CA, USA) coupled to a API 5000™ mass spectrometer (Applied Biosystems Inc., Carlsbad, CA, USA). SA and JA were quantified by liquid chromatography using an Agilent 1200 Series HPLC system (Agilent Technologies) coupled to an API 3200 mass spectrometer (Applied Biosystems).

Data acquisition and processing were conducted using Analyst 1.5 software (Applied Biosystems), and individual hormone levels were quantified against the signal from their corresponding internal standard.

Root Growth and Plant Biomass

Same-age plants were removed from their growth cells and second-generation crown roots were dissected into their lateral and parent roots. After measuring the length of the parent roots, all root samples were dried for 48 h at 55 °C to obtain a dry mass distribution of lateral and parent root tissue. The remaining root mass and aboveground mass were also dried to obtain total biomass distributions.

Statistical Analysis

Data were subjected to Student's t test for unpaired samples, assuming an unequal variance. Statistical significance levels were assigned to the following rating scale: $*P < 0.05$; $**P < 0.01$; $***P < 0.001$.

Results

Leaf Photosynthesis

Exogenous application of IAA and SA to the roots had opposite effects on leaf physiological responses. There was a significant decrease in carbon input (measured as $^{11}CO_2$ fixation) from the IAA treatment, whereas there was a

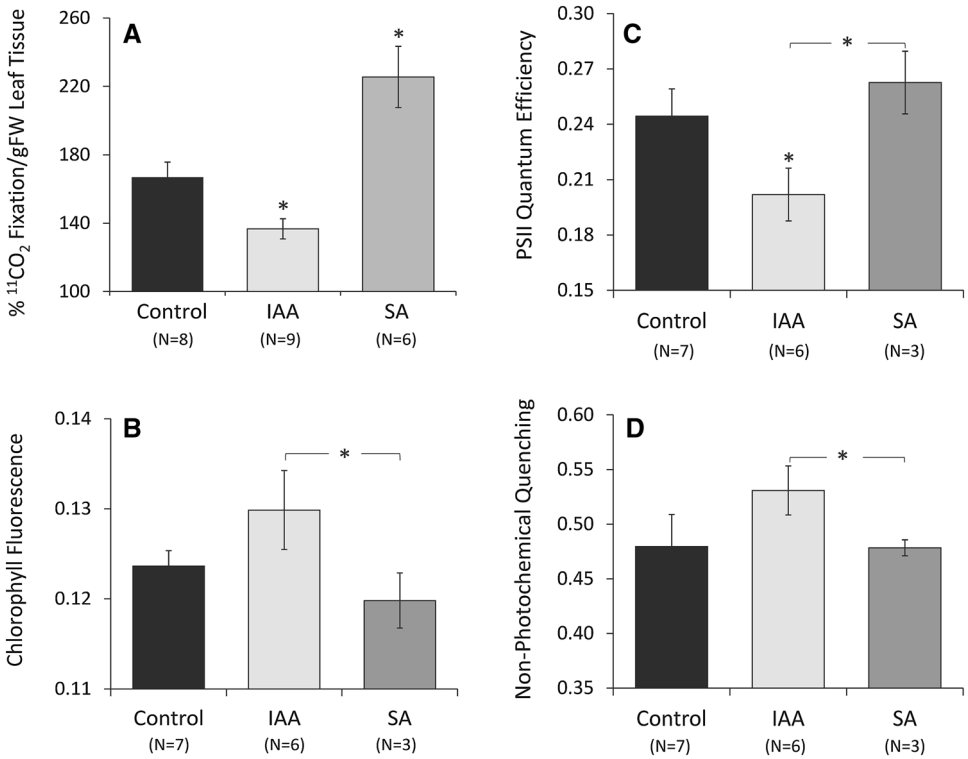

Fig. 2 Leaf photosynthesis parameters measured as a function of root treatments: control (untreated), IAA treated, and SA treated. **a** Percentage of $^{11}CO_2$ fixed by the load leaf normalized to gram fresh weight (gFW) of leaf tissue enclosed within the leaf cell. **b** Total leaf chlorophyll fluorescence. **c** Leaf PSII quantum efficiency. **d** Leaf NPQ. All *bars* are mean values ± SE. $*P < 0.05$ shows significance of the effect of treatment. Comparison of data across IAA and SA root treatments showed statistically different behavior for the three light reaction parameters measured (F_T, PSII, and NPQ)

significant increase from the SA treatment (Fig. 2a) relative to the controls. Complementing this behavior, leaf chlorophyll fluorescence was slightly elevated with IAA and slightly depressed with SA (Fig. 2b). Though these trends were not significant relative to controls, they were significant when compared across treatment types. Leaf PSII levels (Fig. 2c) were significantly decreased with IAA treatment relative to controls, and only slightly elevated with SA. A comparison across IAA and SA treatments revealed significant differences in PSII levels. Changes in leaf NPQ (Fig. 2d) with treatment matched those in chlorophyll fluorescence (Fig. 2b), and these trends were significant across treatments. Note that with the light reactions (comprising *F*, PSII, and NPQ) there is continual competition among the three components (Saura and Quiles 2009). Hence, changes in one component are often reflected by opposite changes in the other two components.

Resource Allocation

IAA significantly decreased leaf export of ^{11}C-photosynthates, whereas SA increased leaf export of ^{11}C-photosynthates (Fig. 3a) relative to the controls. As $^{11}CO_2$ was fixed into the source leaf, this metric indicated the extent to which new carbon (as ^{11}C) was exported out of that tissue to support the growth in distal tissues. Our results also showed that allocation of ^{11}C-photosynthates to belowground roots was reduced in IAA-treated plants (Fig. 3b), whereas SA treatment had no effect on ^{11}C-photosynthates allocation between above- and belowground tissues (Fig. 3b). Finally, our results showed that the speed of ^{11}C-photosynthate transport within roots was significantly slower in IAA-treated roots than in untreated controls but was significantly higher in SA-treated roots (Fig. 3c).

Carbohydrate Metabolism

IAA and SA had different effects on plant sugar metabolism. Specific sugars (sucrose, glucose, and fructose) were analyzed for both short-term ^{11}C and steady-state ^{12}C partitioning using source leaf tissue. Under IAA treatment, there was a significant increase in ^{11}C partitioning into sucrose at the expense of partitioning into glucose and fructose sugars relative to controls. Contrary to this, SA treatment exerted no effect on the ^{11}C fluxes into these sugar metabolite pools (Fig. 4a). For the ^{12}C sugars, our results showed that IAA treatment had no effect on the "size" of the individual sugar pools relative to controls. Contrary to this, SA treatment significantly increased the ^{12}C-sucrose and ^{12}C-glucose pools (Fig. 4b).

IAA and SA had different effects on leaf starch accumulation. Under IAA treatment, there was a significant increase in leaf ^{12}C-starch levels relative to controls (Fig. 5). Contrary to this, SA treatment resulted in decreased ^{12}C-starch levels relative to controls.

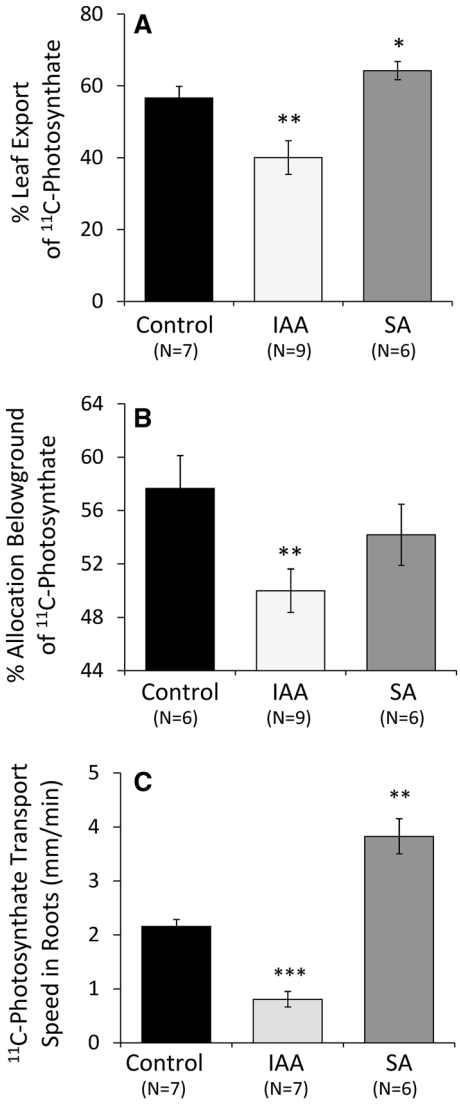

Fig. 3 Whole-plant physiology parameters measured as a function of root treatments: control (untreated), IAA treated, and SA treated. **a** Percentage of ^{11}C-photosynthates exported by the load leaf following treatment. **b** Percentage of ^{11}C-photosynthates allocated to maize roots. **c** Transport speed of ^{11}C-photosynthates allocated to maize roots. All *bars* are mean values ± SE. $***P < 0.001$, $**P < 0.01$, and $*P < 0.05$ show significance of the effect of treatment

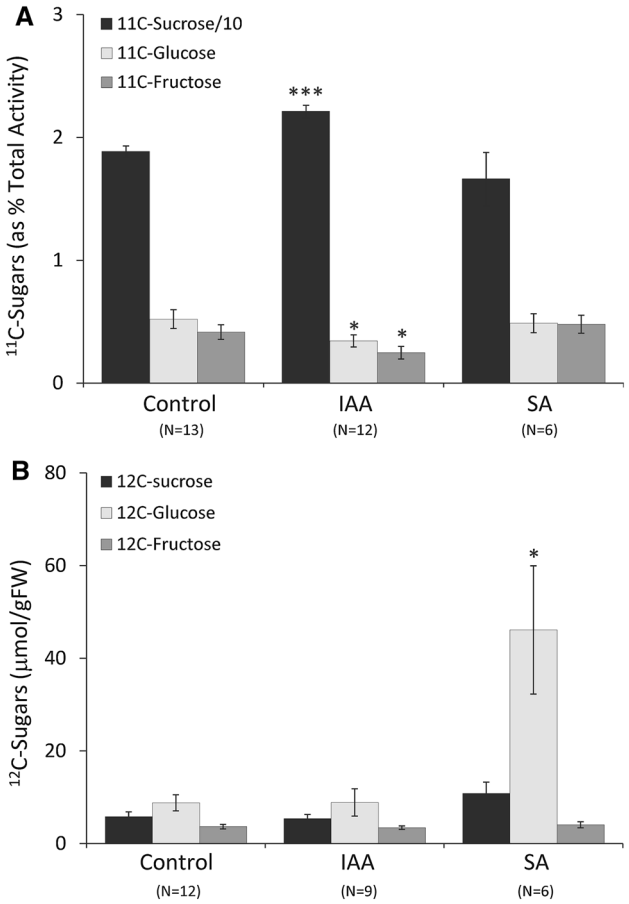

Fig. 4 Metabolic partitioning of plant carbon into nonstructural carbohydrate pools measured as a function of root treatments: control (untreated), IAA treated, and SA treated. **a** Partitioning of ^{11}C into soluble sugars from the maize source leaf. Yields presented as % of load leaf ^{11}C activity, including soluble extracts and insoluble tissue. ^{11}C-sucrose data were divided by 10 for scaling purposes. **b** ^{12}C-soluble sugar concentrations per gram of fresh weight (gFW) of load leaf tissue. All *bars* are mean values ± SE. $***P < 0.001$, $**P < 0.01$, and $*P < 0.05$ show significance of the effect of treatment

Root Growth and Plant Biomass

As seen in the photographs and accompanying radiographic images (Fig. 6), IAA and SA had opposite effects on root growth and root architecture. These differences in growth were reflected by a significantly higher lateral root sink strength for ^{11}C-photosynthate in IAA-treated roots (Fig. 6a), but no change was observed in lateral root sink strength in SA-treated roots. IAA treatment significantly increased the mass ratio of lateral roots to parent root relative to controls (Fig. 6b). SA treatment had no effect on this ratio. IAA treatment significantly decreased root length relative to controls (Fig. 6c). Contrary to this, SA treatment significantly increased root length. Taken together, IAA treatment altered the proportionality of the root tissues, whereas SA treatment did not, it only altered the overall size of the root biomass. However, from the radiographic images it appears that SA promoted growth of lateral roots further down along the length of their parent root.

Overall, IAA treatment decreased biomass of both above- and belowground tissues relative to controls (Fig. 7) and SA treatment increased biomass of both above- and belowground tissues.

Root Hormones

Levels of the endogenous concentrations of plant hormones IAA, SA, and JA were measured in targeted root zones

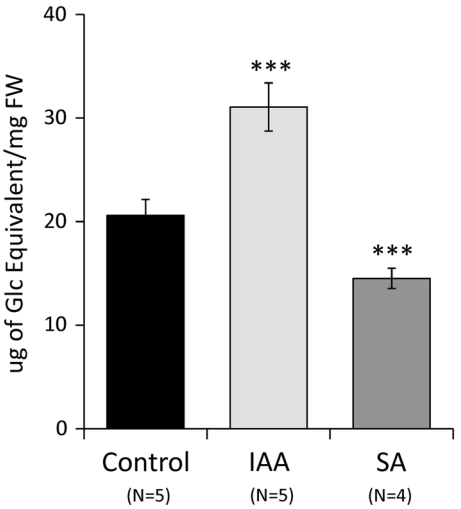

Fig. 5 Starch levels in source leaves as a function of root treatments: control (untreated), IAA treated, and SA treated. Starch levels expressed as micrograms of glucose equivalents of digested starch per milligram fresh weight (mgFW) of tissue. All *bars* are mean values ± SE, where *** denotes a significance of the effect of treatment with $P < 0.001$

(proximal, 6–12 cm; middle, 2–6 cm; and tip, 0–2 cm) for soil-grown control plants (uninfested), and for plants subjected to 4 days of root herbivory by 12 *D. virgifera* larvae at their second instar stage of development (Fig. 8). Damage by feeding *D. virgifera* significantly increased free IAA levels in the middle root zone and root tip relative to controls, but no change was observed in the upper proximal root zone. Contrary to this, herbivore damage significantly increased free SA levels in the proximal zone, but no change was observed in the middle zone or root tip. We also measured levels of JA in all three root zones because it is well known that antagonistic crosstalk exists between JA and SA (Thaler and others 2012). Herbivore damage did not alter the levels of free JA in all three root zones.

Discussion

Overall, our study demonstrated that the phytohormones IAA and SA have opposite effects on plant physiology, plant metabolism, root architecture, and total plant growth in maize. The changes that we observed in root architecture with SA treatment corresponded well with those seen in earlier studies. In one report, the SA treatment resulted in increased root elongation and increased shoot growth in *Glycine max* (L.) (Gutierrez-Coronado and others 1998). In a second report, SA treatment resulted in increased root cap size and caused the appearance of lateral roots closer to the root tip in *Catharanthus roseus* (Echevarria-Machado and others 2007). We note that the increase in root length promoted by SA treatment in our studies did not alter the proportionality of the root system's lateral and parental root mass, it just increased their overall size and lateral root placement (that is, lateral root placement appeared further down along the parent root). These observations were further supported by our observation that relative lateral root sink strength in SA-treated plants appeared unchanged from controls. The observed growth traits in SA-treated roots had a beneficial effect on the overall growth characteristics by enhancing the total plant biomass. This is consistent with a prior study that showed a similar growth enhancement in maize (Tuna and others 2007).

The increased plant growth that we observed in this study with SA treatment was positively correlated with increased carbon input via leaf $^{11}CO_2$ fixation, which matched the increase observed in the PSII quantum efficiency, and correlated with increased ^{11}C-photosynthate transport, which presumably provided the necessary carbon resources to support this enhanced growth rate in distal tissues. However, the lack of change in resource allocation between root types and between above- and belowground tissues with SA treatment may be explained by the fact that root system proportionality (defined by the proportion of lateral root mass relative to the parent root mass) and the relative aboveground/belowground proportionality were unaffected by the SA treatment, and therefore the relative strength of the roots as a sink for resources was unchanged.

Contrary to this, IAA's ability to alter root system proportionality in a drastic way resulted in significant decreases in overall plant growth. The change observed in root architecture as a function of IAA treatment (that is, enhanced lateral root mass) is similar to what was reported by others (McSteen 2010). This change in growth morphology, favoring increased lateral root growth, was correlated with an increase in lateral root sink strength for carbon resources, though total root mass sink strength was suppressed. These effects correlated well with the observed decrease in carbon input matched by a decrease in PSII quantum efficiency, as well as by a decrease in leaf export of ^{11}C-photosynthates and a decrease in their transport to roots.

The inhibition of plant growth with sustained IAA treatment is new. The relationship between IAA and growth can be complicated. For example, there have been several observations that growth stimulation by exogenous application of IAA occurs for only a short time, even when the supply of hormone is continuous (Hall and others 1985; Carrington and Esnard 1988). In fact, detailed analyses of this short-term growth stimulation in maize coleoptiles (Iino 1996) and in pea internodes (Haga and Iino 1997, 1998) suggest that the responsiveness of these tissues to the hormone declines over time.

Finally, our results showed that SA and IAA treatments had different effects on plant carbohydrate metabolism.

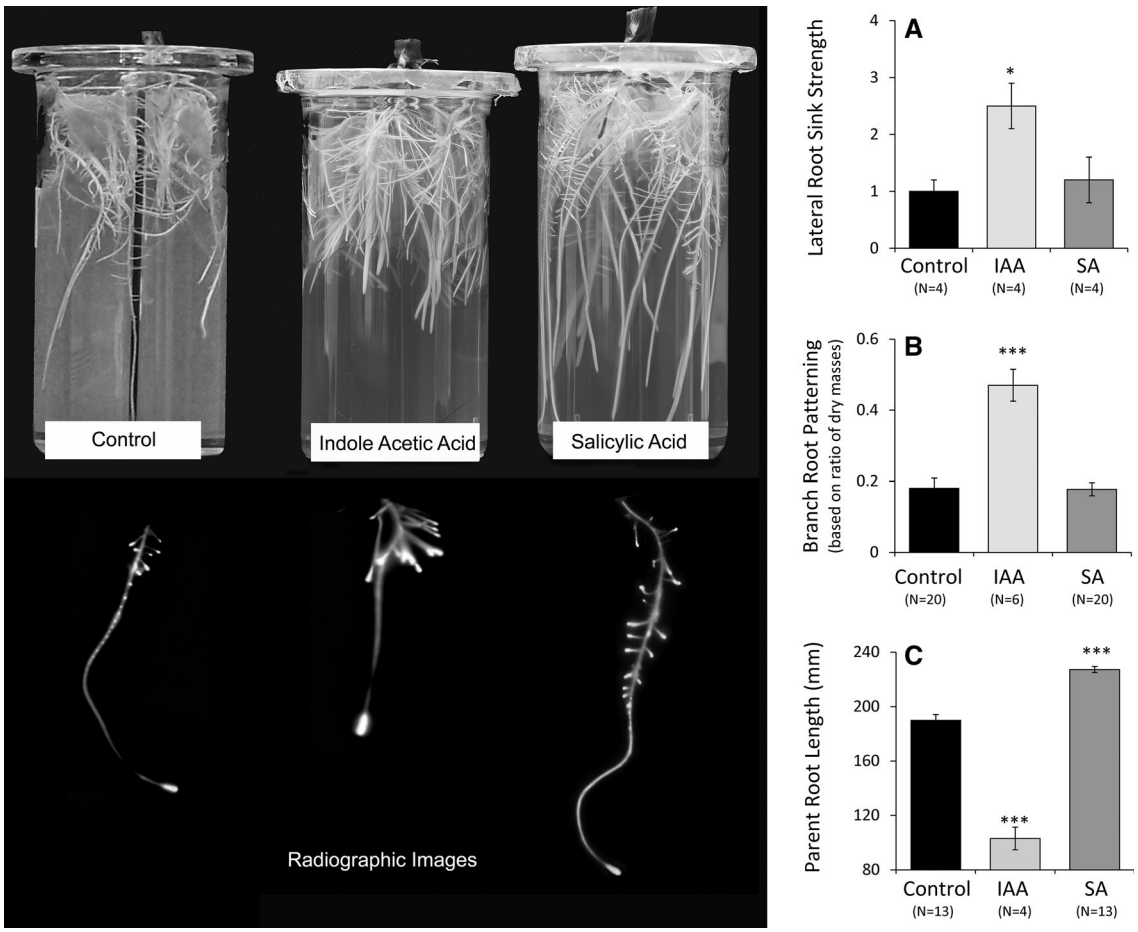

Fig. 6 Photographs in upper panel show typical root for control (untreated), IAA-treated, and SA-treated plants. The *lower panel* presents radiographic images of individual crown roots showing ^{11}C-photosynthate distribution as a function of root treatments. **a**, **b** Root growth parameters measured as a function of root treatments: control (untreated), IAA treated, and SA treated. **a** Relative lateral root sink strength for ^{11}C-photosynthate as calculated using Eq. 5. **b** Branch root ratio was calculated as the ratio of lateral root dried masses to their respective parent root dried mass. **c** Parent root length (mm) was measured from the same roots from which lateral root mass measurements were made. All bars are mean values ± SE. $***P < 0.001$, $**P < 0.01$, and $*P < 0.05$ show the significance of the effect of treatment

The combined information on ^{11}C and ^{12}C isotopic signatures within the individual sugar pools gave us insight into the input flux of newly fixed carbon (as ^{11}C) into the carbohydrate metabolic machinery, as well as the steady-state efflux of ^{12}C into metabolic sinks like starch. We attempted to capture this idea in a conceptual model reflecting carbon influx and carbon efflux, both of which can affect the size of the soluble sugar pool (Fig. 9). We portrayed this model in the context of our results shown in Figs. 4 and 5 (noting that the size of the arrows in this model is a reflection of the magnitude of carbon flux, and the size of the sugar pool is a reflection of the measured concentration when the sampling was carried out).

Of course, this model would predict that with high starch storage, plant growth would be slowed, and with low starch storage, plant growth would be increased to balance carbon efflux from the sugar pools. In fact, starch metabolism is increasingly viewed as important in the coordination of carbon resources for growth (Cross and others 2006; Smith and Stitt 2007; Gibon and others 2009; Graf and others 2010). Recent metabolomics studies in *Arabidopsis* demonstrated a negative correlation between leaf starch levels and growth (Sulpice and others 2009). Furthermore, a past study demonstrated a direct association between SA and starch content. *Arabidopsis* mutants (*cpr1-1*, *cpr5-1*, *cpr6-1*, and *dnd1-1*) with high levels of endogenous SA consistently exhibited lower starch content when compared to wild-type (Col-0) (Mateo and others 2006). These facts fit the expectations of our proposed model on how the individual hormones might impact carbon fluxes into the carbohydrate pools and how this might affect overall plant growth.

Based on our overall findings here, we hypothesized that root-herbivore pressure elicited by *D. virgifera* attack will

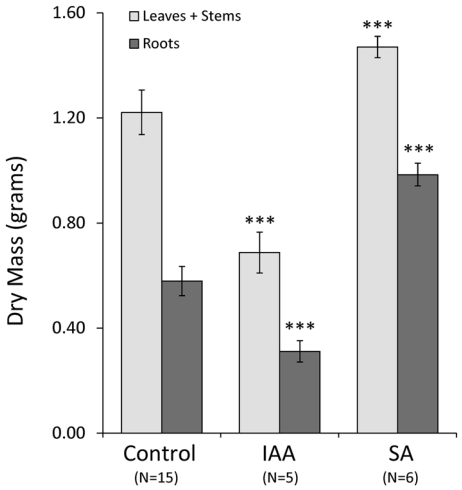

Fig. 7 Total plant biomass measured as a function of root treatments: control (untreated), IAA treated, and SA treated. Data reported as dry biomass (in gram) for the roots and stems + leaves in maize. All *bars* are mean values ± SE. ***$P < 0.001$ shows the significance of the effect of treatment

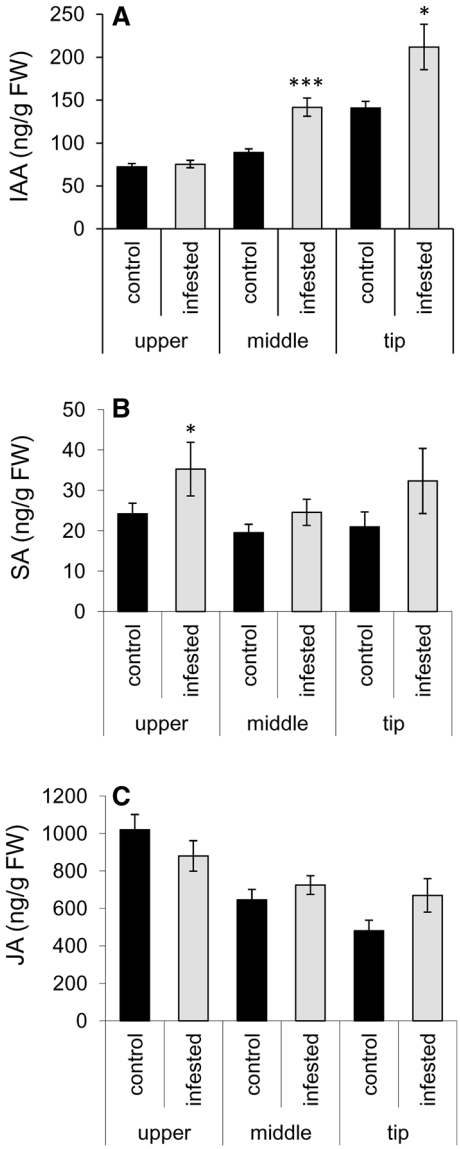

Fig. 8 Levels of the endogenous plant hormones IAA, SA, and JA were measured in nanograms of hormone per gram fresh weight of root tissue (ng gFW^{-1}). Targeted root zones included proximal (6–12 cm), middle (2–6 cm), and tip (0–2 cm). Comparisons were made in soil-grown control plants (uninfested) and in plants subjected to 4 days of root infestation by 12 root worm larvae at their second instar stage of growth. All *bars* are mean values ± SE. ***$P < 0.001$, **$P < 0.01$, and *$P < 0.05$ show the significance of the effect of treatment

alter the levels of IAA and/or SA in the roots, possibly in opposite directions. We know from past research that such stress increases the concentration of sucrose in maize roots while decreasing glucose levels, as well as increases local and systemic root levels of the amino acid tryptophan (Robert and others 2012), one of the essential resources for the biosynthesis of IAA (Ljung and others 2005; McSteen 2010). Indeed, our results show significant differences in the patterning of IAA and SA upon herbivory. These differences are not attributed to known antagonistic behavior between JA and SA as the JA levels were unchanged (Thaler and others 2012). These findings demonstrate that root herbivory differentially affects IAA and SA in maize roots, which may lead to local and systemic changes in the plant's metabolism. This observation is contrary to what was observed in wheat seedlings which are also monocots (Shakirova and others 2003). There, treatment with SA increased IAA endogenous levels. Taking into account spatiotemporal changes in hormone homeostasis will be important to come to biologically relevant conclusions that translate across plant species and place hormone regulation in the context of plant–herbivore interactions.

In summary, radiotracer research in plant biology has provided new insight into the opposing effects that IAA and SA hormones can have in shaping root growth and whole-plant growth. Under stress-free growth conditions for this grass system, our data provide evidence that SA promotes plant growth with increased carbon input to support this increased growth in both above- and belowground tissues. Of course, these studies were carried out in a setting where the plant roots received a continual and homogeneous supply of both water and nutrients via the agar gel growth medium, so plants were not stressed by limiting resources. It would be interesting to know how nutrient and water stress affects root morphology and what role IAA and SA play under these stress conditions to promote plant growth. In the broader scope, these studies are a first step toward providing new knowledge for designing hardier crops for energy and agriculture capable of sustainable growth in a continually changing environment.

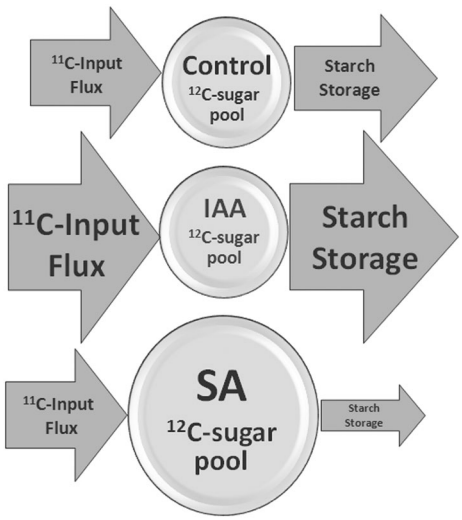

Fig. 9 Conceptual model of hormone treatment effects on carbohydrate pools through regulation of input metabolic flux of new carbon and its outflow to storage

Acknowledgments This article has been authored by Brookhaven Science Associates, LLC under contract number DE-AC02-98CH10886 with the U.S. Department of Energy (DOE), which supported R. A. Ferrieri in this effort. Additional support was provided by a DOE training grant through the University of Missouri and Brookhaven National Laboratory (Grant No. DE-SC0002040), which supported L. Song; the DOE SULI Program, which supported B. Agtuca; the German Academic Exchange Service (Deutscher Akademischer Austauschdienst, DAAD) Bonn, which supported E. Rieger and K. Hilger; a Marie Curie Intra-European Fellowship (Grant No. 273107), which supported M. Erb; a Swiss National Foundation Fellowship (Grant No. 140196), which supported C. Robert; and a USDA-DOE (Grant No. 2012-BNL-MO094-BUDG), which supported A. Karve. The United States Government retains and the publisher, by accepting the article for publication, acknowledges that the United States Government retains a nonexclusive, paid-up, irrevocable, world-wide license to publish or reproduce the published form of this manuscript, or allow others to do so, for United States Government purposes. The authors give a special thanks to M. Schueller for his assistance in isotope production and to D. Alexoff for his assistance in image analysis. Finally, the authors thank the USDA for supplying germplasm accessions of the B73 line through their National Plant Germplasm Service.

References

Babst BA, Karve A, Judt T (2013) Radio-metabolite analysis of carbon-11 biochemical partitioning to non-structural carbohydrates for integrated metabolism and transport studies. Plant Cell Physiol 54:1016–1025

Baker DB, Ray PM (1965) Direct and indirect effect of auxin on cell wall synthesis in oat coleoptile tissue. Plant Physiol 40:345–352

Buchanan BB, Gruissem W, Jones RL (2000) Biochemistry and molecular biology of plants, 1st edn. Wiley, New York, p 558

Cahill JF Jr, McNickle GG (2011) The behavioral ecology of nutrient foraging by plants. Annu Rev Ecol Evol Syst 42:289–311

Carrington CMS, Esnard J (1988) The elongation response of watermelon hypocotyls to indole-3-acetic acid: a comparative study of excised segments and intact plants. J Exp Bot 39:441–450

Cross JM, Von Korff M, Altmann T, Bartzetko L, Sulpice R, Gibon Y, Paalacios N, Stitt M (2006) Variation of enzyme activities and metabolite levels in 24 *Arabidopsis* accessions growing in carbon-limited conditions. Plant Physiol 142:1574–1588

Durrant WE, Dong X (2004) Systemic acquired resistance. Ann Rev Phytopathol 24:185–209

Echevarria-Machado I, Escobedo RM, Larque-Saavedra A (2007) Responses of transformed *Catharanthus roseus* roots to femtomolar concentrations of salicylic acid. Plant Phyiol Biochem 45:501–507

Ferrieri RA, Wolf AP (1983) The chemistry of positron emitting nucleogenic atoms with regards to preparation of labeled compounds of practical utility. Radiochim Acta 34:69–83

Ferrieri RA, Gray D, Babst B, Schueller M, Schlyer D, Thorpe MR, Orians CM, Lerdau M (2005) Use of carbon-11 in *Populus* shows that exogenous jasmonic acid increases biosynthesis of isoprene from recently fixed carbon. Plant, Cell Environ 28:591–602

Ferrieri AP, Agtuca B, Appel H, Ferrieri RA, Schultz JC (2012) Getting to the root of the problem: methyl jasmonate induces temporal changes in carbon transport and partitioning in *Arabidopsis thaliana* that depend on root–shoot signaling. Plant Physiol 161:692–704

Gibon Y, Pyle ET, Sulpice R, Lunn JE, Hohne M, Gunther M, Stitt M (2009) Adjustment of growth, starch turnover, protein content and central metabolism to a decrease of carbon supply when *Arabidopsis* is grown in very short photoperiods. Plant, Cell Environ 32:859–874

Graf A, Schlereth A, Stitt M, Smith AM (2010) Circadian control of carbohydrate availability for growth in *Arabidopsis* plants at night. Proc Natl Acad Sci USA 107:9458–9463

Gutierrez-Coronado MA, Trejo-Lopez C, Larque-Saavedra A (1998) Effects of salicylic acid on the growth of roots and shoots in soybean. Plant Phyiol Biochem 36:563–565

Haga K, Iino M (1997) The short-term growth stimulation induced by external supply of IAA in internodes of intact pea seedlings. Aust J Plant Physiol 24:215–226

Haga K, Iino M (1998) Auxin-growth relationships in maize coleoptiles and pea internodes and control by auxin of the tissue sensitivity to auxin. Plant Physiol 117:1473–1486

Hall JL, Brummell DA, Gillespie J (1985) Does auxin stimulate the elongation of intact plant stems? New Phytol 100:341–345

Hayat S, Ali B, Ahmad A (2007) Salicylic acid—A plant hormone chap. 1. Springer, New York, pp 1–14

Hodge A (2004) The plastic plant: root responses to heterogeneous supplies of nutrients. New Phytol 162:9–24

Iino M (1996) Short-term stimulation of growth induced by the apical application of IAA to intact maize coleoptiles. Plant Cell Physiol 37:27–33

Kang HG, Singh KB (2000) Characterization of salicylic acid-responsive, *Arabidopsis* Dof domain proteins: overexpression of OBP3 leads to growth defects. Plant J 21:329–339

Katagiri F (2004) A global view of defense gene expression regulation—a highly interconnected signaling network. Curr Opin Plant Biol 7:506–511

Kazan K, Manners JM (2009) Linking development to defense: auxin in plant–pathogen interactions. Trends Plant Sci 14:373–382

Klaus R, Fisher W, Hauck E (1989) Use of a new adsorbent in the separation and detection of glucose and fructose by HPTLC. Chromatographia 28:364–366

Klaus R, Fisher W, Hauck HE (1990) Application of a thermal in situ reaction for fluorometric detection of carbohydrates on NH_2-layers. Chromatographia 29:467–472

Kumar B, Abdel-Ghani AH, Reyes-Matamoros J, Hochholdinger F, Lubberstedt T (2012) Genotypic variation of root architecture traits in seedlings of maize (*Zea mays* L.) inbred lines. Plant Breeding 131:465–478

Kunkel BN, Brooks DM (2002) Cross-talk between signaling pathways in pathogen defense. Curr Opin Plant Biol 5:325–331

Li L, Li L (1995) Effects of resorcinol and salicylic acid on the formation of adventitious roots on hypocotyl cutting of *Vigna radiate*. J Trop Subtrop Bot 3:67–71

Ljung K, Hull AK, Celenza J, Yamada M, Estelle M, Normanly J, Sandberg G (2005) Sites and regulation of auxin biosynthesis in *Arabidopsis* roots. Plant Cell 17:1090–1104

Llorente F, Muskett P, Vallet-Sanches A, Lopez G, Ramos B, Sanches-Rodriguez C, Jorda L, Parker J, Molina A (2008) Repression of the auxin response pathway increases *Arabidopsis* susceptibility to necrotrophic fungi. Mol Plant 1:496–509

Machado RAR, Ferrieri AP, Robert CAM, Kallenbach M, Baldwin IT, Erb M (2013) Leaf-herbivore attack reduces carbon reserves and regrowth from the roots via jasmonate and auxin signaling. New Phytol. doi:10.1111/nph.12438

Mateo A, Funck D, Muhlenbock P, Kular B, Mullineaux PM, Karpinski S (2006) Controlled levels of salicylic acid are required for optimal photosynthesis and redox homeostasis. J Exp Bot 57:1795–1807

McSteen P (2010) Auxin and monocot development. Cold Spring Harb Perspect Biol 2(3):a001479

Minchin PEH, Thorpe MR (2003) Using the short-lived isotope ^{11}C in mechanistic studies of photosynthate transport. Funct Plant Biol 30:831–841

Park JE, Park JU, Kim YS, Staswick PE, Jeon J, Yun J, Kim SY, Kim J, Lee YH, Park CM (2007) GH3-mediated auxin homeostasis links growth regulation with stress adaptation response in *Arabidopsis*. J Biol Chem 282:10036–10046

Rasmann S, Köllner TG, Degenhardt J, Hiltpold I, Toepfer S, Kuhlmann U, Gershenzon J, Turlings TCJ (2005) Recruitment of entomopathogenic nematodes by insect-damaged maize roots. Nature 434:732–737

Rivas-San VM, Plasencia J (2011) Salicylic acid beyond defense: its role in plant growth and development. J Exp Bot 62:3321–3338

Robert CAM, Erb M, Hibbard BE, French BW, Zwahlen C, Turlings TCJ (2012) A specialist root herbivore reduces plant resistance and uses an induced plant volatile to aggregate in a density-dependent manner. Funct Ecol 26:1429–1440

Saura P, Quiles MJ (2009) Assessment of photosynthesis tolerance to herbicides, heat and high illumination by fluorescence imaging. Open Plant Sci J 3:7–13

Shah J (2003) The salicylic acid loop in plant defense. Curr Opin Plant Biol 6:365–371

Shakirova FM, Sakhabutdinova AR, Bezrukova MV, Fathkutdinova RA, Fathkutdinova DR (2003) Changes in the hormonal status of wheat seedlings induced by salicylic acid and salinity. Plant Sci 164:317–322

Smith AM, Stitt M (2007) Coordination of carbon supply and plant growth. Plant, Cell Environ 30:1126–1149

Spoel SH, Dong X (2008) Making sense of hormone crosstalk during plant immune responses. Cell Host Microbe 3:348–351

Sulpice R, Pyle ET, Ishihara H, Trenkamp S, Steinfath M, Witucka-Wall H, Gibon Y, Usadel B, Poree F, Piques MC, Von Korff M, Steinhauser MC, Keurentjes JJB, Guenther M, Hoehne M, Selbig J, Fernie AR, Altmann T, Stitt M (2009) Starch as a major integrator in the regulation of plant growth. Proc Natl Acad Sci USA 106:10348–10353

Thaler JS, Humphrey PT, Whiteman NK (2012) Evolution of jasmonate and salicylate signal crosstalk. Trends Plant Sci 17:260–270

Thorpe MR, Ferrieri AP, Herth MM, Ferrieri RA (2007) Imaging transport of methyl jasmonate and photoassimilate: jasmonate moves in both phloem and xylem and restores sugar transport after proton transport is decoupled. Planta 226:541–551

Truman W, Bennett MH, Kubigsteltig I, Turnbull C, Grant M (2007) *Arabidopsis* systemic immunity uses conserved defense signaling pathways and is mediated by jasmonates. Proc Natl Acad Sci USA 104:1075–1080

Tuna AL, Kaya C, Dikilitas M, Yokas I, Burun B, Altunlu H (2007) Comparative effects of various salicylic acid derivatives on key growth parameters and some enzyme activities in salinity stressed maize (*Zea Mays* L.) plants. Pak J Bot 39:787–798

Vadassery J, Reichelt M, Hause B, Gershenzon J, Boland W, Mithofer A (2012) CML42-mediated calcium signaling coordinates responses to Spodoptera herbivory and abiotic stresses in *Arabidopsis*. Plant Physiol 159:1159–1175

Vlot AC, Dempsey DMA, Klessig DF (2009) Salicylic acid, a multifaceted hormone to combat disease. Annu Rev Phytopathol 47:177–206

Wasternack C (2007) Jasmonates: an update on biosynthesis, signal transduction and action in plant stress response, growth and development. Ann Bot 100:681–697

Woodward AW, Bartel B (2005) Auxin: regulation, action, and interaction. Ann Bot 95:707–735

Zhang Z, Li Q, Li Z, Staswick PE, Wang M, Zhu Y, He Z (2007) Dual regulation role of GH3.5 in salicylic acid and auxin signaling during *Arabidopsis–Pseudomonas syringae* interaction. Plant Physiol 145:450–464